

# Spectroscopic conductivity imaging of a cell culture

Habib Ammari<sup>a,\*</sup>, Laure Giovangigli<sup>b</sup>, Hyeuknam Kwon<sup>c</sup>,  
Jin-Keun Seo<sup>c</sup> and Timothée Wintz<sup>d</sup>

<sup>a</sup> *Department of Mathematics, ETH Zürich, Rämistrasse 101, CH-8092 Zürich, Switzerland*  
E-mail: [habib.ammari@math.ethz.ch](mailto:habib.ammari@math.ethz.ch)

<sup>b</sup> *Department of Mathematics, University of California at Irvine, 340 Rowland Hall, Irvine, California 92697-3875, USA*  
E-mail: [lgiovang@uci.edu](mailto:lgiovang@uci.edu)

<sup>c</sup> *Department of Computational Science and Engineering, Yonsei University, 50 Yonsei-Ro, Seodaemun-Gu, Seoul 120-749, Korea*  
E-mails: [3c273-85@daum.net](mailto:3c273-85@daum.net), [seoj@yonsei.ac.kr](mailto:seoj@yonsei.ac.kr)

<sup>d</sup> *Department of Mathematics and Applications, Ecole Normale Supérieure, 45 Rue d'Ulm, 75005 Paris, France*  
E-mail: [timothee.wintz@ens.fr](mailto:timothee.wintz@ens.fr)

**Abstract.** In this paper, we present a simplified electrical model for tissue culture. We derive a mathematical structure for overall electrical properties of the culture and study their dependence on the frequency of the current. We introduce a method for recovering the microscopic properties of the cell culture from the spectral measurements of the effective conductivity. Numerical examples are provided to illustrate the performance of our approach.

Keywords: cell culture, conductivity properties, spectroscopic conductivity measurements, inverse homogenization

## 1. Introduction

Cell culture production processes, such as those from stem cell therapy, must be monitored and controlled to meet strict functional requirements. For example, a cell culture of cartilage, designed to replace that in the knee, must be organized in a specific way.

Hyaline cartilage is located on the joint surface and play an important role in body movement. In normal articular cartilage, there is a depth-dependent stratified structure known as zonal organization. As a simplified model, cartilage comprises three different layers [10]: a superficial zone in outer 10%, a middle zone that is 50% of the height, and a deep zone consisting in the inner 40%. At the microscopic level, cartilage tissue is composed of cells, collagen fibers, and glycosaminoglycans (GAGs). The concentration and organization of each microstructure differs among the three layers. In the superficial zone, cells are anisotropic and horizontally aligned, collagen orientation is also horizontal and GAGs have a lower concentration than in the other layers. In the middle zone, there are fewer cells and they are isotropic, collagen is randomly oriented and there is a medium concentration of GAGs. In the deep zone, cells are isotropic, cell density is higher than in the middle zone, collagen is vertically aligned and

---

\*Corresponding author. E-mail: [habib.ammari@math.ethz.ch](mailto:habib.ammari@math.ethz.ch).

there is a high GAG density. As these parameters all contribute to the function of collagen in the knee, and must be replicated in the cell culture.

It is important that the method for monitoring cell cultures is non-destructive. Destructive methods require hundreds of samples to be cultured for a single functional tissue, and for the samples to be monitored multiple times during maturation. Here, we propose a microscopic electrical impedance tomography (micro-EIT) method for monitoring cell cultures that exploits the distinctive dielectric properties of cells and other microstructures. In this method, electrodes inject a current into the medium at different frequencies and the corresponding dielectric potentials are recorded, thus enabling reconstruction of the microscopic parameters of the medium. The parameters of interest are cell density, collagen orientation, and GAG density, as well as the orientation and shape of cells.

EIT uses a low-frequency current (below 500 kHz) to visualize the internal impedance distribution of a conducting domain such as a tissue sample or the human body. Recent studies measured electrical conductivity values and anisotropy ratios of engineered cartilage to distinguish extracellular matrix samples containing differing amounts of collagen and GAGs. During chondrogenesis over a six-week period, these measurements could distinguish the stages of the process and provide information regarding the internal depth-dependent structure.

In this work, we provide a mathematical framework for determining the microscopic properties of the cell culture from spectral measurements of the effective conductivity. For simplicity, we consider a microstructure comprising two components in a background medium. One of the components has a frequency dependent on the material parameters arising from the cell membrane structure, while the other has constant conductivity and permittivity over the frequency range. First, we derive in Theorem 2 the overall electrical properties of the culture, which depend on the volume fraction of each component and associated membrane polarization tensors defined by (10) and (11). Then, we show that the spectral measurements of the overall electrical properties of the culture can be used to determine the volume fraction of each component and the anisotropy ratio of the first component. For doing so, we study the dependence of the membrane polarization tensors on the operating frequency and use the spectral theorem to recover in Proposition 9 from the measurement of the effective conductivity on a range of frequencies the coefficients of its expansion with respect to the frequency. Proposition 9 also provides the anisotropy ratio of the cell culture.

This paper is organized as follows. In Section 2, we present a simplified model of the tissue culture. In Section 3, we derive an equivalent effective conductivity for the solution at the macroscopic scale. In Section 4, we present a method based on spectral measurements, in which microscopic properties are measured from the effective conductivity. This process is known as inverse homogenization or dehomogenization [5,14]. Finally, we provide some numerical examples to illustrate our main findings.

## 2. The direct problem

In this section, we propose a simple electrical model for the tissue and derive an effective conductivity using periodic homogenization.

### 2.1. Problem setting

We consider the domain of interest – the cell culture – to be described by a domain  $\Omega \subset \mathbb{R}^3$ . We assume that  $\Omega = D \times (0, 1)$  where  $D \subset \mathbb{R}^2$  denotes a floor of the culture medium; see Fig. 1. Following

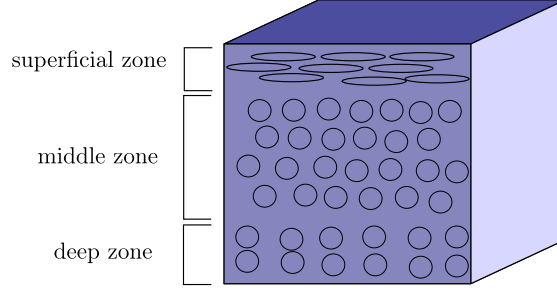


Fig. 1. Organization of the cells in the cartilage tissue.

[11,17,18], we describe the conductivity of the medium by a scalar field

$$\sigma_{\omega,\epsilon}(x) = \sigma_{\omega}\left(x, \frac{x}{\epsilon}\right),$$

where  $\omega$  denotes the angular frequency of the injected current, and  $\epsilon > 0$  is a small parameter representing the microscopic scale of the medium;  $\sigma$  is 1-periodic in every direction in the second variable. Let us consider the following unit domain:

$$\mathcal{Y} = \left(-\frac{1}{2}; \frac{1}{2}\right)^d.$$

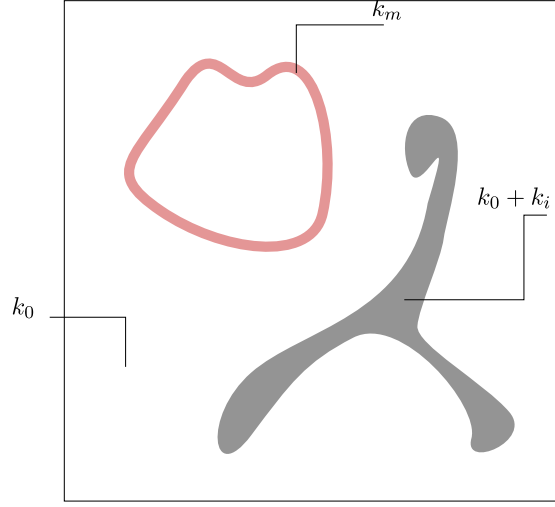
For a fixed  $x$ ,  $\sigma(x, \frac{x}{\epsilon})$  describes the conductivity in a single cartilage tissue with cell size  $\epsilon$  at a location  $x \in \Omega$ . To have a complete model of the tissue,  $\sigma$  must describe the conductivity of both cells and of the other inclusions, i.e., collagen and GAGs. The biological fluid conductivity is noted  $k_0$  and is assumed to be frequency independent. The cells are made of biological fluid enclosed in a very thin and very resistive membrane [2] of thickness  $\epsilon\delta$  for some small parameter  $\delta > 0$ . The conductivity of the membrane is frequency dependent and is noted  $k_m(\omega)$ . The cell shape varies slowly with the parameter  $x \in \Omega$  compared to the microscale  $\epsilon$ . The other inclusions are described by some frequency independent conductivity function  $k_i(x, \frac{x}{\epsilon})$ . Let

$$\psi : \Omega \times \mathbb{R}^d \rightarrow \mathbb{R}$$

be a  $C^1(\Omega \times \mathbb{R}^d)$  function, 1-periodic in every direction with respect to the second variable. We assume that the function  $\psi$  is the level set function for the membrane boundary given by  $\Omega_{\epsilon}^+ = \{x : \psi(x, \frac{x}{\epsilon}) > \delta\}$  (resp.  $\Omega_{\epsilon}^- = \{x : \psi(x, \frac{x}{\epsilon}) < -\delta\}$ ). We also assume that the support of  $k_i(x, y)$  is strictly included in  $\{(x, y) : \psi(x, y) > \delta\}$ . We can now describe the conductivity  $\sigma_{\omega}$ , which is schematically represented at a fixed  $x$  in Fig. 2:

$$\sigma_{\omega}(x, y) = \begin{cases} k_0 + k_i(x, y) & \text{if } \psi(x, y) > \delta, \\ k_0 & \text{if } \psi(x, y) < -\delta, \\ k_m(\omega) & \text{else.} \end{cases} \quad (1)$$

Now that we have an expression for the conductivity in the medium, as commonly accepted in EIT, we use the quasistatic approximation for the electrical potential. For an input current  $g(x) \sin(\omega t)$  on the

Fig. 2. Typical values of  $\sigma_\omega$  on  $\mathcal{Y}$ .

boundary  $\partial\mathcal{Y}$ , with  $\int_{\partial\Omega} g = 0$ , the real part of the corresponding time-harmonic potential, denoted by  $u_{\omega,\epsilon}$ , satisfies the following problem approximately:

$$\begin{cases} \nabla \cdot \sigma_{\omega,\epsilon} \nabla u_{\omega,\epsilon} = 0 & \text{in } \Omega, \\ \sigma_{\omega,\epsilon} \nabla u_{\omega,\epsilon} \cdot \nu = g & \text{on } \partial\Omega. \end{cases} \quad (2)$$

where  $\nu$  is the outer normal vector on  $\partial\Omega$ . Here, we impose the normalization  $\int_{\Omega_\epsilon} u_{\omega,\epsilon} = 0$ .

**Remark 1.** Let us briefly explain how the expression of  $\sigma_\omega$  in (1) is derived. We should note that the frequency dependent behaviors of  $\sigma_{\omega,\epsilon}$  in (2) are attributed to thin cell membranes. Imagine that we inject an oscillating current at the angular frequency  $\omega$  into the cube  $\mathcal{Y}$ . Then, the resulting time-harmonic potential  $w = u + iv$  in  $\mathcal{Y}$  is governed by

$$\nabla \cdot ((\sigma'(y) + i\omega\sigma''(y))\nabla w(y)) = 0 \quad \text{for } y \in \mathcal{Y},$$

where  $\sigma'$  denotes the conductivity distribution and  $\sigma''$  is the permittivity distribution in  $\mathcal{Y}$ . In [9], it was shown that, under some conditions on the membrane, the real part  $u$  approximately satisfies

$$\nabla \cdot \left( \frac{|\sigma' + i\omega\sigma''|^2}{\sigma'} \nabla u \right) = 0 \quad \text{in } \mathcal{Y}. \quad (3)$$

Since  $\sigma'' \ll \sigma'$  outside the membrane, we have

$$\frac{|\sigma' + i\omega\sigma''|^2}{\sigma'} \approx \sigma' \quad \text{outside the membrane.}$$

Hence, it is reasonable to assume that the conductivity outside the membrane, as a coefficient of the elliptic PDE (3), does not change with frequency. On the other hand, since  $\sigma'$  on the membrane is very

small, the effect of  $\sigma''$  is not negligible. Hence, the conductivity,  $k_m$ , on the membrane changes with frequency as follows:

$$\frac{|\sigma' + i\omega\sigma''|^2}{\sigma'} = \sigma' + \frac{\omega^2\sigma''}{\sigma'} \quad \text{on the membrane.}$$

## 2.2. Homogenization of the tissue

We are now interested in getting rid of the microscale oscillations of  $\sigma_{\omega,\epsilon}$ , since boundary measurements will only allow us to image macroscale variations of the conductivity. To this end, we proceed to the homogenization of equation (2). Assume that  $k_0 + k_i$  is bounded from below and from above:

$$0 < \underline{\sigma} \leq k_0 + k_i \leq \bar{\sigma}.$$

From [2], we have two-scale convergence [1,11,13] of  $u_{\omega,\epsilon}$  to  $u_\omega$ , which is a solution to

$$\begin{cases} \nabla \cdot \sigma_\omega^* \nabla u_\omega = 0 & \text{in } \Omega, \\ \sigma_\omega^* \nabla u_\omega \cdot \nu = g & \text{on } \partial\Omega, \\ \int_\Omega u_\omega = 0, \end{cases} \quad (4)$$

for an input current  $g(x) \sin(\omega t)$  on the boundary  $\partial\Omega$ . Here,  $\sigma_\omega^*$  is called the effective conductivity which can be represented by [2]

$$\begin{aligned} \sigma_\omega^*(x) e_p \cdot e_q &= \int_{\mathcal{Y}} \sigma_\omega(x, y) \nabla(y_p + v_p(y)) \cdot e_q dy, \quad \forall p, q \in \{1, \dots, d\} \\ &= k_0 \left( \delta_{p,q} + \int_{\partial\mathcal{Y}} \frac{\partial v_p}{\partial \nu} y_q ds(y) \right), \end{aligned} \quad (5)$$

where  $e_p := (0, \dots, 1, \dots, 0)$  with 0 components except  $p$ th component 1, and  $v_p$  is the solution to the following equation on  $\mathcal{Y}$  for  $p = 1, \dots, d$ :

$$\begin{cases} \nabla \cdot (\sigma_\omega(x, y) \nabla(v_p(y) + y_p)) = 0 & \text{for } y \in \mathcal{Y}, \\ v_p & \text{1-periodic,} \\ \int_{\mathcal{Y}} (v_p(y) + y_p) dy = 0. \end{cases} \quad (6)$$

As  $\delta \rightarrow 0$ ,  $v_p$  can be approximated [8,15,16] by the solution of the following equation, where  $\beta(\omega) = \frac{\delta}{k_m(\omega)}$ :

$$\begin{cases} \nabla \cdot (\sigma_\omega(x, y) \nabla(v_p(y) + y_p)) = 0 & \text{for } y \in \mathcal{Y} \setminus \partial C, \\ k_0 \frac{\partial}{\partial \nu} (v_p^+(y) + y_p) = k_0 \frac{\partial}{\partial \nu} (v_p^-(y) + y_p) & \text{for } y \in \partial C, \\ v_p^+(y) - v_p^-(y) = \beta(\omega) k_0 \frac{\partial}{\partial \nu} (v_p^+(y) + y_p) & \text{for } y \in \partial C, \\ v_p & \text{1-periodic,} \\ \int_{\mathcal{Y}} v_p(y) + y dy = 0. \end{cases} \quad (7)$$

Here,  $\partial C$  denotes the membrane of the cell  $C$  and  $\beta k_0$  is the effective thickness of the membrane.

### 3. Imaging the microstructure from effective conductivity measurements

In this section, we do not care about the space dependence of  $\sigma_\omega^*$ , and will therefore drop it. We will thus assume that  $\sigma_\omega^*$  is constant equal to some matrix in  $\mathcal{M}_d(\mathbb{C}) := \{m \in \mathbb{C}^{d \times d} : m_{i,j} = m_{j,i} \text{ for } i, j = 1, 2, \dots, d\}$ . We will show what kind of information on the microstructure we can recover from the knowledge of  $\sigma_\omega^*$  in a range of frequencies  $\omega \in (\omega_1, \omega_2)$ . First, in Section 3.1, we will obtain a simple representation of the effective conductivity in the dilute case, where the volume fraction of both cells and other inclusions is small compared to the volume of biological fluid. Then, in the following sections we will use this representation and will show how to recover information about the microstructure using the spectral measure.

#### 3.1. Effective conductivity in the dilute case

Here, we consider some reference cell  $C_0$  and some reference inclusion  $B_0$  with there  $C^2$  boundaries  $\partial C_0$  and  $\partial B_0$ . We assume that  $C = x_C + \rho_C C_0$  and  $\beta(\omega) = \rho_C \beta_0(\omega)$  for some reference  $\beta_0(\omega)$  and let  $B = x_B + \rho_B B_0$ , where  $x_C$  and  $x_B$  respectively indicate the locations of the cell and inclusion and  $\rho_C$  and  $\rho_B$  their characteristic sizes. We assume that the conductivity  $k_i$  of the inclusion is given by

$$k_i(y) = (k_0 - k_1)\chi_B(y),$$

where  $\chi_B$  denotes the characteristic function of  $B$ .

The effective conductivity is therefore expressed as

$$\sigma_\omega^* e_p \cdot e_q = \int_{\mathcal{Y}} \sigma(y) \nabla(y_p + v_p(y)) \cdot e_q dy, \quad \forall p, q \in \{1, \dots, d\},$$

where, for  $p \in \{1, \dots, d\}$ ,

$$\left\{ \begin{array}{ll} \nabla \cdot (k_0 \nabla(v_p(y) + y_p)) = 0 & \text{in } \mathcal{Y} \setminus (B \cup \partial C), \\ \nabla \cdot (k_1 \nabla(v_p(y) + y_p)) = 0 & \text{in } B, \\ k_0 \frac{\partial}{\partial \nu}(v_p^+(y) + y_p) = k_0 \frac{\partial}{\partial \nu}(v_p^-(y) + y_p) & \text{on } \partial C, \\ v_p^+ - v_p^- = \beta(\omega) k_0 \frac{\partial}{\partial \nu}(v_p^+(y) + y_p) & \text{on } \partial C, \\ v_p^+ - v_p^- = 0 & \text{on } \partial B, \\ k_0 \frac{\partial}{\partial \nu}(v_p^+(y) + y_p) = k_1 \frac{\partial}{\partial \nu}(v_p^-(y) + y_p) & \text{on } \partial B, \\ v_p & \text{periodic,} \\ \int_{\mathcal{Y}} (v_p(y) + y) dy = 0. & \end{array} \right. \quad (8)$$

From now on,  $\mathcal{I}$  denotes the inclusion map  $H^{1/2}(\partial C) \rightarrow H^{-1/2}(\partial C)$ , where  $H^{1/2}$  and  $H^{-1/2}$  are the Sobolev spaces of order 1/2 and  $-1/2$  on  $\partial C$ . We will now proceed to prove the following result.

**Theorem 2.** *Let  $f_k = \rho_k^d$ ,  $k \in \{B, C\}$  and  $f = \max(f_B, f_C)$ . Then we have the following expansion:*

$$\sigma_\omega^* = k_0 [I + f_B M_{B_0} + f_C M_{C_0}(\omega)] + o(f), \quad (9)$$

where

$$M_{C_0}(\omega)e_p \cdot e_q = \int_{\partial C_0} v_q(y) \left( \frac{1}{\beta_0(\omega)k_0} \mathcal{I} + \mathcal{L}_{\#,C_0} \right)^{-1} [v_p](y) ds(y), \quad (10)$$

and

$$M_{B_0}e_p \cdot e_q = \int_{\partial B_0} (\lambda I - \mathcal{K}_{\#,B_0}^*)^{-1} [v_p](y) y_q ds(y) \quad (11)$$

with

$$\lambda = \frac{k_1 + k_0}{2(k_1 - k_0)}.$$

We begin by reviewing properties of periodic layer potentials. Let us define the periodic Green's function

$$G_{\#}(x) = - \sum_{n \in \mathbb{Z}^d \setminus \{0\}} \frac{e^{2i\pi n \cdot x}}{4\pi^2 |n|^2}.$$

Thanks to Poisson's summation formula, in the sense of distribution,  $G_{\#}$  satisfies

$$\Delta G_{\#}(x) = \sum_{n \in \mathbb{Z}^d} \delta(x - n) - 1. \quad (12)$$

We write  $G_{\#}(x, y) := G_{\#}(x - y)$ . Let us introduce the periodic single layer potential, for a Lipschitz domain  $D \subset \mathcal{Y}$ :

$$\begin{aligned} \mathcal{S}_{\#,D} : H^{-1/2}(\partial D) &\rightarrow H_{\text{loc}}^1(\mathbb{R}^d \setminus \partial D) \\ \varphi &\mapsto x \mapsto \int_{\partial D} G_{\#}(x, y) \varphi(y) ds(y), \end{aligned}$$

the periodic double layer potential

$$\begin{aligned} \mathcal{D}_{\#,D} : H^{1/2}(\partial D) &\rightarrow H_{\text{loc}}^1(\mathbb{R}^d \setminus \partial D) \\ \varphi &\mapsto x \mapsto \int_{\partial D} \frac{\partial G_{\#}}{\partial \nu(y)}(x, y) \varphi(y) ds(y), \end{aligned}$$

and the periodic Neumann–Poincaré operator

$$\begin{aligned} \mathcal{K}_{\#,D} : H^{1/2}(\partial D) &\rightarrow H^{1/2}(\partial D) \\ \varphi &\mapsto x \mapsto \int_{\partial D} \frac{\partial G_{\#}}{\partial \nu(y)}(x, y) \varphi(y) ds(y), \end{aligned}$$

and its adjoint given by

$$\begin{aligned} \mathcal{K}_{\#,D}^* : H^{-1/2}(\partial D) &\rightarrow H^{-1/2}(\partial D) \\ \varphi &\mapsto x \mapsto \int_{\partial D} \frac{\partial G_{\#}}{\partial \nu(x)}(x, y) \varphi(y) ds(y). \end{aligned}$$

We review the jump properties of the layer potentials [3].

**Lemma 3.** *We have the following jump relations along the boundary  $\partial D$ :*

$$\begin{aligned} \mathcal{S}_{\#,D}[\varphi](x)|_+ &= \mathcal{S}_{\#,D}[\varphi](x)|_-, \\ \frac{\partial}{\partial \nu} \mathcal{S}_{\#,D}[\varphi](x)|_{\pm} &= \left( \pm \frac{1}{2} I + \mathcal{K}_{\#,D}^* \right) [\varphi](x), \\ \mathcal{D}_{\#,D}[\varphi](x)|_{\pm} &= \left( \mp \frac{1}{2} I + \mathcal{K}_{\#,D} \right) [\varphi](x), \\ \frac{\partial}{\partial \nu} \mathcal{D}_{\#,D}[\varphi](x)|_+ &= \frac{\partial}{\partial \nu} \mathcal{D}_{\#,D}[\varphi](x)|_-. \end{aligned}$$

where the subscript  $\pm$  means  $f_D(x)|_{\pm} = \lim_{t \rightarrow 0^+} f_D(x \pm t\nu(x))$  for  $x \in \partial D$ .

We denote by  $\mathcal{L}_{\#,D}$  the operator  $\varphi \mapsto \frac{\partial}{\partial \nu} \mathcal{D}_{\#,D}[\varphi]$ . We write  $\nu_p = \nu \cdot e_p$  on  $\partial B$  and  $\partial C$ . Using these jump relations, we have the following representation theorem for  $\nu_p$ ,  $p \in \{1, \dots, d\}$ .

**Theorem 4.** *We have the following representation for  $\nu_p$ :*

$$\nu_p = C_p + \mathcal{S}_{\#,B}[\varphi_{1,p}] - \mathcal{D}_{\#,C}[\varphi_{2,p}], \quad (13)$$

where  $C_p$  is a constant and  $(\varphi_1, \varphi_2)$  satisfies the following system:

$$\begin{cases} (\lambda I - \mathcal{K}_{\#,B}^*)[\varphi_{1,p}] + \frac{\partial}{\partial \nu} \mathcal{D}_{\#,C}[\varphi_{2,p}] = \nu_p & \text{on } \partial B, \\ \left( \frac{1}{\beta k_0} \mathcal{I} + \mathcal{L}_{\#,C} \right) [\varphi_{2,p}] - \frac{\partial}{\partial \nu} \mathcal{S}_{\#,B}[\varphi_{1,p}]|_+ = \nu_p & \text{on } \partial C. \end{cases} \quad (14)$$

**Lemma 5.** *For any  $(F, G) \in H^{-1/2}(\partial B) \times H^{-1/2}(\partial C)$ , the system*

$$\begin{cases} (\lambda I - \mathcal{K}_{\#,B}^*)[\varphi_1] + \frac{\partial}{\partial \nu} \mathcal{D}_{\#,C}[\varphi_2] = F & \text{on } \partial B, \\ \left( \frac{1}{\beta k_0} \mathcal{I} + \mathcal{L}_{\#,C} \right) [\varphi_2] - \frac{\partial}{\partial \nu} \mathcal{S}_{\#,B}[\varphi_1]|_+ = G & \text{on } \partial C, \end{cases}$$

admits a unique solution  $(\varphi_1, \varphi_2) \in H^{-1/2}(\partial B) \times H^{1/2}(\partial C)$ .

**Proof.** As shown in the Appendix,  $\frac{1}{\beta} \mathcal{I} + \mathcal{L}_{\#,C}$  and  $\lambda I - \mathcal{K}_{\#,B}^*$  are invertible for  $\lambda \notin (-1/2, 1/2]$ . Moreover, since

$$\frac{\partial}{\partial \nu} \mathcal{D}_{\#,C} : H^{1/2}(\partial C) \rightarrow H^{-1/2}(\partial B)$$



and

$$\frac{\partial}{\partial v} \mathcal{S}_{\#,B} : H^{-1/2}(\partial B) \rightarrow H^{-1/2}(\partial C)$$

are compact, the operator

$$H^{-1/2}(\partial \Omega) \times H^{1/2}(\partial \Omega) \rightarrow H^{-1/2}(\partial \Omega) \times H^{-1/2}(\partial \Omega)$$

$$(\varphi_1, \varphi_2) \mapsto \left( (\lambda I - \mathcal{K}_{\#,B}^*)[\varphi_1] - \frac{\partial}{\partial v} \mathcal{D}_{\#,C}[\varphi_2], \left( \frac{1}{\beta k_0} \mathcal{I} + \mathcal{L}_{\#,C} \right)[\varphi_2] - \frac{\partial}{\partial v} \mathcal{S}_{\#,B}[\varphi_1] \Big|_+ \right)$$

is a Fredholm operator. It is therefore sufficient to show that it is injective. Let  $(\varphi_1, \varphi_2)$  be such that

$$\begin{cases} (\lambda I - \mathcal{K}_{\#,B}^*)[\varphi_1] + \frac{\partial}{\partial v} \mathcal{D}_{\#,C}[\varphi_2] = 0 & \text{on } \partial B, \\ \left( \frac{1}{\beta k_0} \mathcal{I} + \mathcal{L}_{\#,C} \right)[\varphi_2] - \frac{\partial}{\partial v} \mathcal{S}_{\#,B}[\varphi_1] = 0 & \text{on } \partial C. \end{cases}$$

Let  $v = \mathcal{S}_{\#,B}[\varphi_1] - \mathcal{D}_{\#,C}[\varphi_2]$ . Then  $v$  is 1-periodic in every direction, and  $v$  is a solution by construction to the following problem:

$$\begin{cases} \nabla \cdot (k_0 \nabla (v_p(y) + y)) = 0 & \text{for } y \in \mathcal{Y} \setminus (B \cup \partial C), \\ \nabla \cdot (k_1 \nabla (v_p(y) + y)) = 0 & \text{for } y \in B, \\ k_0 \frac{\partial}{\partial v} (v_p^+(y) + y) = k_0 \frac{\partial}{\partial v} (v_p^-(y) + y) & \text{for } y \in \partial C, \\ v_p^+(y) - v_p^-(y) = \beta(\omega) k_0 \frac{\partial}{\partial v} (v_p^+(y) + y) & \text{for } y \in \partial C, \\ v_p^+(y) - v_p^-(y) = 0 & \text{for } y \in \partial B, \\ k_0 \frac{\partial}{\partial v} (v_p^+(y) + y) = k_1 \frac{\partial}{\partial v} (v_p^-(y) + y) & \text{for } y \in \partial B. \end{cases} \quad (15)$$

By the uniqueness of the solution to (15) up to a constant,  $v(x) = c, \forall x \in \mathcal{Y}$ . Then, we have  $\varphi_1 = 0$  on  $\partial C$  and  $\varphi_2 = 0$  on  $\partial B$  because they are equal to the jumps of  $v$  (resp.  $\frac{\partial v}{\partial v}$ ) across  $\partial B$  (resp.  $\partial C$ ). This concludes the proof.  $\square$

We can now proceed to prove Theorem 4.

**Proof.** Let  $(\varphi_1, \varphi_2)$  be a solution of (14), and let

$$v_p = \mathcal{S}_{\#,B}[\varphi_1] - \mathcal{D}_{\#,C}[\varphi_2].$$

Then using the jump relations of the layer potentials, we have that  $v_p$  is a solution of (8), except that we have not necessarily  $\int_{\partial \mathcal{Y}} v_p = 0$ . We just have to adjust  $C_p$  accordingly.  $\square$

We now proceed to compute the representation of the effective conductivity.

**Theorem 6.** *We have the following representation for  $\sigma_\omega^*$ :*

$$\sigma_\omega^* = k_0(I + M^*),$$

where  $M^* = (M_{pq}^*)_{p,q=1}^d$  is defined by

$$(M^*)_{pq} = \int_{\partial B} x_p \varphi_{1,q} ds - \int_{\partial C} v_p \varphi_{2,q} ds, \quad \forall p, q \in \{1, \dots, d\}.$$

**Proof.** We recall the expression of  $\sigma_\omega^*$  in (5):

$$\sigma_\omega^* e_p \cdot e_q = k_0 \left( \delta_{p,q} + \int_{\partial \mathcal{Y}} \frac{\partial v_p}{\partial \nu}(y) y_q ds(y) \right).$$

Using representation (13), we obtain

$$\int_{\partial \mathcal{Y}} \frac{\partial v_p}{\partial \nu}(y) y_q ds(y) = \int_{\partial \mathcal{Y}} \frac{\partial \mathcal{S}_{\#,B}[\varphi_{1,p}]}{\partial \nu}(y) y_q ds(y) - \int_{\partial \mathcal{Y}} \frac{\partial \mathcal{D}_{\#,C}[\varphi_{2,p}]}{\partial \nu}(y) y_q ds(y)$$

and

$$\begin{aligned} \int_{\partial \mathcal{Y}} \frac{\partial \mathcal{S}_{\#,B}[\varphi_{1,p}]}{\partial \nu}(y) y_q ds(y) &= \int_{\partial B} \frac{\partial \mathcal{S}_{\#,B}[\varphi_{1,p}]}{\partial \nu} \Big|_+ (y) y_q ds(y) - \int_{\partial B} \frac{\partial \mathcal{S}_{\#,B}[\varphi_{1,p}]}{\partial \nu} \Big|_- (y) y_q ds(y) \\ &= \int_{\partial B} y_q \varphi_{1,p}(y) ds(y). \end{aligned}$$

The same reasoning applies to the second part of the equation:

$$\begin{aligned} \int_{\partial \mathcal{Y}} \frac{\partial \mathcal{D}_{\#,C}[\varphi_{2,p}]}{\partial \nu}(y) y_q ds(y) &= \int_{\partial C} \mathcal{D}_{\#,C}[\varphi_{2,p}]|_+(y) v_q(y) ds(y) - \int_{\partial C} \mathcal{D}_{\#,C}[\varphi_{2,p}]|_-(y) v_q(y) ds(y) \\ &= \int_{\partial C} \varphi_{2,p}(y) v_q(y) ds(y). \end{aligned}$$

Therefore,

$$\begin{aligned} \sigma_\omega^* e_p \cdot e_q &= k_0 \left( \delta_{p,q} + \int_{\partial \mathcal{Y}} \frac{\partial v_p}{\partial \nu}(y) y_q ds(y) \right) \\ &= k_0 \left( \delta_{p,q} + \int_{\partial B} y_q \varphi_{1,p}(y) ds(y) - \int_{\partial C} \varphi_{2,p} v_q(y) ds(y) \right). \end{aligned} \quad \square$$

We turn to the proof of Theorem 2. We first review asymptotic properties of the periodic Green's function  $G_\#$ . The following result from [3, Chapter 2] holds.

**Lemma 7.** *We have the following expansion for  $G_\#$ :*

$$G_\#(x) = G(x) + R_d(x),$$

where  $G$  is the Green function and  $R_d$  is a smooth function on  $\mathbb{R}^d$  and its Taylor expansion at 0 is given by

$$R_d(x) = R_d(0) - \frac{1}{2d}|x|^2 + O(|x|^4). \quad (16)$$

Using this expansion, we obtain by exactly the same arguments as those in [3, Chapter 8] the following expansion, which is uniform in  $z \in \partial B_0$ ,

$$\begin{aligned} (\lambda I - \mathcal{K}_{B_0}^*)[\psi_{B,p}](z) &= v_{B_0,p}(z) + o(1) \\ \left( \frac{1}{\beta_0 k_0} \mathcal{I} + \mathcal{L}_{C_0} \right) [\psi_{C,p}](z) &= v_{C_0,p}(z) + o(1), \end{aligned}$$

where  $\mathcal{K}_{B_0}^*$  is the standard Neumann–Poincaré operator and  $\mathcal{L}_{C_0}$  denotes the operator  $\frac{\partial}{\partial \nu} \mathcal{D}_{C_0}$  associated with the standard double layer potential  $\mathcal{D}_{C_0}$ :

$$\begin{aligned} \mathcal{K}_{B_0}^*[\phi](x) &:= \int_{\partial B_0} \frac{\partial G}{\partial \nu(x)}(x, y) \phi(y) ds(y), \\ \mathcal{L}_{C_0}[\phi](x) &:= \frac{\partial}{\partial \nu} \int_{\partial C_0} \frac{\partial G}{\partial \nu(y)}(x, y) \phi(y) ds(y). \end{aligned}$$

Therefore, we arrive at the result stated in Theorem 2.

### 3.2. Spectral measure of the tissue

Expansion (9) yields

$$\sigma_\omega^* = k_0 [I + \rho_B^d M_{B_0} + \rho_C^d M_{C_0}(\omega)] + O(\rho^d)$$

with

$$M_{C_0}(\omega) e_p \cdot e_q = \int_{\partial C_0} v_q(y) \left( \frac{1}{\beta_0(\omega) k_0} \mathcal{I} + \mathcal{L}_{C_0} \right)^{-1} [v_p](y) ds(y).$$

In order to use the spectral theorem in a Hilbert space, we have to modify the expression of  $M_{C_0}$ . Let  $\mathcal{L}_{C_0}^{-1}$  be the inverse of  $\mathcal{L}_{C_0} : H_0^{1/2}(\partial C_0) \rightarrow H_0^{-1/2}(\partial C_0)$ . Then we write

$$\left( \frac{1}{\beta_0(\omega) k_0} \mathcal{I} + \mathcal{L}_{C_0} \right)^{-1} [v_p] = \left( \frac{1}{\beta_0(\omega) k_0} \mathcal{L}_{C_0}^{-1} \circ \mathcal{I} + I_{H^{1/2}} \right)^{-1} \mathcal{L}_{C_0}^{-1} [v_p].$$

The following result holds.

**Lemma 8.**  $\mathcal{L}_{C_0}^{-1} \circ \mathcal{I}$  can be extended to a self-adjoint operator  $\mathcal{L}^\dagger : L^2(\partial C_0) \rightarrow L^2(\partial C_0)$ , whose image is a subset of  $H^{1/2}(\partial C_0)$ .

**Proof.** Let  $\mathcal{J}_1 : L^2(\partial C_0) \hookrightarrow H^{-1/2}(\partial C_0)$  and  $\mathcal{J}_2 : H^{1/2}(\partial C_0) \hookrightarrow L^2(\partial C_0)$ . Let  $\mathcal{L}^\dagger = \mathcal{J}_2 \circ \mathcal{L}_{C_0}^{-1} \circ \mathcal{J}_1$ . Then obviously  $\mathcal{L}^\dagger$  extends  $\mathcal{L}_{C_0}^{-1} \circ \mathcal{I}$  and its image is a subset of  $H^{1/2}(\partial C_0)$ . Let us show that it is self-adjoint. Let  $(\varphi, \psi) \in L^2(\partial C_0) \times L^2(\partial C_0)$ . Let  $\langle \cdot, \cdot \rangle_{L^2}$  and  $\langle \cdot, \cdot \rangle_{H^{1/2}, H^{-1/2}}$  respectively denote the  $L^2$ -scalar product and the duality pairing between  $H^{1/2}(\partial C_0)$  and  $H^{-1/2}(\partial C_0)$ . We have

$$\begin{aligned} \langle \mathcal{L}^\dagger[\varphi], \psi \rangle_{L^2} &= \langle \mathcal{L}_{C_0}^{-1}[\varphi], \psi \rangle_{L^2} = \langle \mathcal{L}_{C_0}^{-1}[\varphi], \psi \rangle_{H^{1/2}, H^{-1/2}} \\ &= \langle \mathcal{L}_{C_0}^{-1}[\psi], \varphi \rangle_{H^{1/2}, H^{-1/2}} = \langle \mathcal{L}_{C_0}^{-1}[\psi], \varphi \rangle_{L^2} = \langle \mathcal{L}^\dagger[\psi], \varphi \rangle_{L^2}, \end{aligned}$$

since  $\mathcal{L}_{C_0}$  is self-adjoint from  $H^{1/2}(\partial C_0)$  onto  $H^{-1/2}(\partial C_0)$ .  $\square$

From this result, we can now proceed. From the spectral theorem, there exists a spectral measure  $E$  such that for any  $z \in \mathbb{C} \setminus \Lambda(\mathcal{L}^\dagger)$  and for any  $(\varphi, \psi) \in (L^2(\partial C_0))^2$ ,

$$\left\langle \left( \frac{\mathcal{L}^\dagger}{z} + I \right)^{-1} [\varphi], \psi \right\rangle_{L^2} = \int_{\Lambda(\mathcal{L}^\dagger)} \frac{1}{\frac{x}{z} + 1} \varphi(x) \psi(x) dE(x), \quad (17)$$

where  $\Lambda(\mathcal{L}^\dagger)$  denotes the spectrum of  $\mathcal{L}^\dagger$ . Let

$$F_{p,q}(z) = \delta_{p,q} + \rho_B^d M_{B_0} e_p \cdot e_q + \rho_C^d \int_{\Lambda(\mathcal{L}^\dagger)} \frac{1}{\frac{x}{z} + 1} \mathcal{L}_{C_0}^{-1}[v_p](x) \cdot v_q(x) dE(x), \quad (18)$$

where  $\delta_{p,q} = 1$  if  $p = q$  and  $\delta_{p,q} = 0$  if  $p \neq q$ . Therefore, we have

$$\sigma_\omega^* e_p \cdot e_q \simeq k_0 [F_{p,q}(\beta_0(\omega)k_0)].$$

Since

$$\lim_{z \rightarrow 0} F(z) = I + \rho_B^d M_{B_0},$$

there is no singularity of  $F$  in 0. Since  $0 \notin \Lambda(\mathcal{L}^\dagger)$ , (17) is valid on a neighborhood of 0.

**Proposition 9.** Let  $F = (F_{p,q})_{p,q=1}^d$  be defined by (18). Then the following expansion of  $F$  in a neighborhood of 0 holds:

$$F_{p,q}(z) = \sum_{k=0}^{\infty} a_{k,p,q} z^k, \quad (19)$$

where

$$a_{0,p,q} = I + \rho_B^d M_{B_0} e_p \cdot e_q,$$

and

$$a_{1,p,q} = \rho_C^d v_p \cdot v_q.$$

**Proof.** Identity (19) holds using the analyticity of  $F$  in a neighborhood of 0. We also have

$$a_{0,p,q} = \lim_{z \rightarrow 0} F_{p,q}(z) = \delta_{p,q} + \rho_B^d M_{B_0} e_p \cdot e_q.$$

In order to obtain the next coefficients, we begin by establishing the following limit:

$$\lim_{z \rightarrow 0} (\mathcal{L}^\dagger + zI)^{-1} [v_p] = \mathcal{L}_{C_0} [v_p], \quad p = 1, 2.$$

Indeed, let  $\varphi(z) = (\mathcal{L}^\dagger + zI)^{-1} [v_p]$ . Then

$$\varphi(z) = \frac{1}{z} (v_p - \mathcal{L}^\dagger \varphi_p).$$

Since the range of  $\mathcal{L}^\dagger$  is a subset of  $H^{1/2}(\partial C_0)$ ,  $\varphi(z) \in H^{1/2}(\partial C_0)$ . Therefore,

$$\varphi(z) = \mathcal{L}_{C_0} [v_p] - z \mathcal{L}_{C_0} [\varphi](z) \xrightarrow{z \rightarrow 0} \mathcal{L}_{C_0} [v_p].$$

This yields

$$\lim_{z \rightarrow 0} \frac{1}{z} (F_{p,q}(z) - F_{p,q}(0)) = \rho_C^d v_p \cdot v_q. \quad \square$$

In the following, we write

$$F(z) = (F_{p,q}(z))_{p,q \in \{1, \dots, d\}}, \quad z \in \mathbb{C} \setminus \Lambda(\mathcal{L}_{C_0}),$$

and

$$A_k = (a_{k,p,q})_{p,q \in \{1, \dots, d\}}, \quad k \in \mathbb{N}. \quad (20)$$

Since  $F_{p,q}$  is analytic on  $\mathbb{C} \setminus \Lambda(\mathcal{L}_{C_0})$ , the values of  $a_k$  can be recovered from the values of  $F_{p,q}$  on a subset of  $\mathbb{C}$  with a limiting point. Therefore, we can reconstruct the values  $a_{k,p,q}$  from the measurements of the effective conductivity  $\sigma_\omega^*$  in a band of frequencies  $\omega \in (\omega_1, \omega_2)$ . Further details on this will be provided in the following section.

## 4. Inverse homogenization

### 4.1. Imaging of the anisotropy ratio

The anisotropy ratio (the ratio between the largest and the lowest eigenvalue of the effective conductivity tensor) depends on the frequency [2]. Furthermore, in the general case, the anisotropy orientation (the direction of the effective conductivity tensor eigenvectors) depends also on the frequency. However, in the special case where we have an axis of symmetry of a single inclusion or a cell, the anisotropy orientation is independent of the frequency.

We denote by  $\mathcal{O}_d(\mathbb{R}) := \{R \in \mathbb{R}^{d \times d} \mid R^T R = 1, \det(R) = 1\}$  the set of rotational matrices. Here, the superscript  $T$  denotes the transpose. For convenience, we write  $R(x) := Rx$  for  $x \in \mathcal{Y}$  and  $R(D) := \{Rx : x \in D\}$ . We will need the following covariance result :

**Lemma 10.** *Let  $R \in \mathcal{O}_d(\mathbb{R})$  and  $f \in L^2(\partial C_0)$ . Then*

$$\mathcal{L}_{C_0}[f \circ R] \circ R = \mathcal{L}_{C_0}[f].$$

**Proof.** We have, for any  $x \in \partial C_0$ ,

$$\mathcal{L}_{C_0}[f \circ R](R(x)) = \lim_{h \rightarrow 0} \nabla \mathcal{D}_{C_0}[f \circ R](R(x) + hv(R(x))) \cdot v(R(x)).$$

Moreover,

$$\begin{aligned} \mathcal{D}_{C_0}[f \circ R](R(x)) &= \int_{\partial C_0} \nabla G(R(x) - y) \cdot v(y) f(R(y)) ds(y) \\ &= \int_{\partial C_0} \nabla G(R(x) - R(y)) \cdot v(R(y)) f(y) ds(y). \end{aligned}$$

Since  $G$  is isotropically symmetric,  $\nabla G(R(x) - y) = R(\nabla G(x - y))$ , therefore for any  $x, y \in \partial C_0$ ,

$$\nabla G(R(x) - R(y)) \cdot v(R(y)) = R(\nabla G(x - y)) \cdot R(v(y)) = \nabla G(x - y) \cdot v(y)$$

so that

$$\mathcal{D}_{C_0}[f \circ R](R(x)) = \mathcal{D}_{C_0}[f](x), \quad \forall x \in \partial C_0.$$

This in turn implies that

$$\begin{aligned} \mathcal{L}_{C_0}[f \circ R](R(x)) &= \lim_{h \rightarrow 0} \nabla \mathcal{D}_{C_0}[f \circ R](R(x) + hv(R(x))) \cdot v(R(x)) \\ &= \lim_{h \rightarrow 0} \nabla \mathcal{D}_{C_0}[f](x + v(x)) \cdot v(x) = \mathcal{L}_{C_0}[f](x). \end{aligned}$$

□

The following corollary holds immediately.

**Corollary 11.** *Let  $R \in \mathcal{O}_d(\mathbb{R})$ . Then,*

$$M_{R(C_0)} = RM_{C_0}R^T.$$

Let us begin with the two-dimensional case.

**Proposition 12.** *Let  $d = 2$ , and  $(\epsilon_1, \epsilon_2)$  be an orthonormal basis of  $\mathbb{R}^2$ ; see Fig. 3. Let  $\xi$  be the orthogonal symmetry of axis  $\epsilon_1$ . If  $\xi(C_0) = C_0$ , then*

$$F(z)\epsilon_1 \cdot \epsilon_2 = 0, \quad \forall z \in \mathbb{C} \setminus \Lambda(\mathcal{L}^\dagger).$$

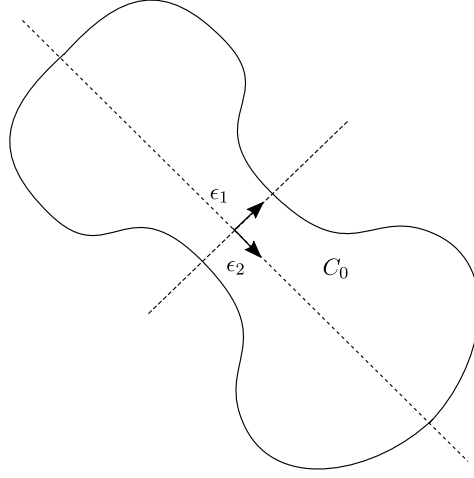


Fig. 3. A domain presenting a symmetry. In this case, the anisotropy direction is frequency independent.

**Proof.** We have

$$\begin{aligned}
 F(z)\epsilon_1 \cdot \epsilon_2 &= \rho_C^d \int_{\partial C_0} \left( \frac{\mathcal{L}^\dagger}{z} + I \right)^{-1} [v \cdot \epsilon_1](x) v(x) \cdot \epsilon_2 ds(x) \\
 &= \rho_C^d \int_{\partial C_0} \left( \frac{\mathcal{L}^\dagger}{z} + I \right)^{-1} [v \cdot \epsilon_1](\xi(x)) v(\xi(x)) \cdot \epsilon_2 ds(x) \\
 &= -\rho_C^d \int_{\partial C_0} \left( \frac{\mathcal{L}^\dagger}{z} + I \right)^{-1} [v \cdot \epsilon_1](x) v(x) \cdot \epsilon_2 ds(x)
 \end{aligned}$$

because  $v(\xi(x)) \cdot \epsilon_1 = v(x) \cdot \epsilon_1$  and  $v(\xi(x)) \cdot \epsilon_2 = -v(x) \cdot \epsilon_2$ . Therefore,

$$F(z)\epsilon_1 \cdot \epsilon_2 = 0, \quad \forall z \in \mathbb{C} \setminus \Lambda(\mathcal{L}^\dagger). \quad \square$$

We have a similar result in three dimensions. The following proposition holds.

**Proposition 13.** *Let  $d = 3$ , and  $(\epsilon_1, \epsilon_2, \epsilon_3)$  be an orthonormal basis of  $\mathbb{R}^3$ . Let  $\xi_1$  (resp.  $\xi_2$ ) be the orthogonal symmetry of axis  $\epsilon_1$  (resp.  $\epsilon_2$ ). If  $\xi_1(C_0) = \xi_2(C_0) = C_0$ , then*

$$F(z)\epsilon_j \cdot \epsilon_k = 0, \quad \forall z \in \mathbb{C}, \forall k \neq j \in \{1, 2, 3\}.$$

**Proof.** The proof is exactly the same as in the  $d = 2$  case and is therefore omitted.  $\square$

**Remark 14.** It is also true that the symmetry axes of  $B_0$  correspond to the eigenvectors of the polarization tensor  $M_{B_0}$ . Therefore, the anisotropy direction of the frequency-independent background can also be recovered as the principal directions of  $M_{B_0}$ .

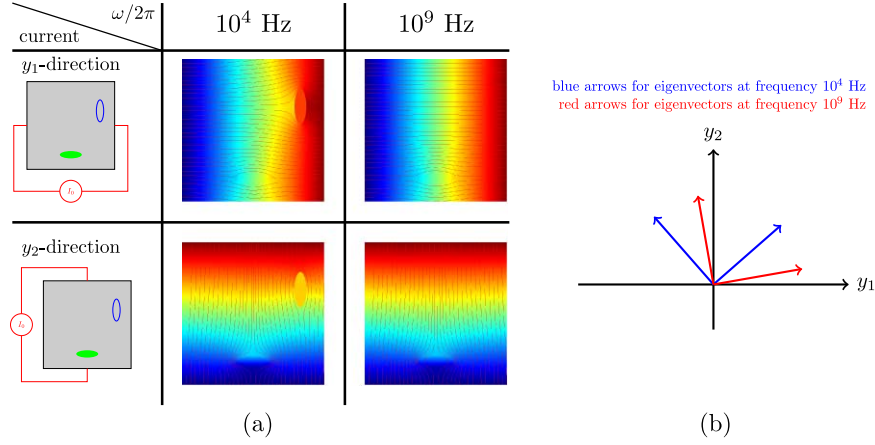


Fig. 4. (a) shows voltage map with current flows for each  $y_1$ - and  $y_2$ -direction current at  $10^4$  and  $10^9$  Hz. (b) shows eigenvectors of the effective conductivity. Blue arrows represent eigenvectors at frequency  $\omega/2\pi = 10^4$  Hz while red arrows are representing eigenvectors at frequency  $\omega/2\pi = 10^9$  Hz.

**Remark 15.** Even if each of inclusion and cell has an axis of symmetry, the direction of eigenvectors of the effective conductivity tensor can be frequency dependent. The following numerical test is conducted to show an example of frequency dependency. There are an ellipsoidal inclusion with major axis  $e_1$  and minor axis  $e_2$  and an ellipsoidal cell with major axis  $e_2$  and minor axis  $e_1$  in the unit square as shown in Fig. 4(a). For the square domain  $\mathcal{Y} = (-\frac{1}{2}, \frac{1}{2})^2$ , each axis length of cell and inclusion is  $1/8$ , and  $1/24$ . The center of ellipsoidal cell and inclusion are  $(1/3, 1/6)$  and  $(0, -1/3)$  respectively. The ratio between membrane thickness and size of a cell is  $5 \times 10^{-3}$ . The conductivity value of medium, membrane, inclusion are  $0.5$  S/m,  $10^{-5}$  S/m, and  $10^{-12}$  S/m respectively. We use (5) to compute the effective conductivity tensor. For the numerical computation, we take advantage of using  $u_j$  satisfying  $\nabla \cdot (\sigma \nabla u_j) = 0$  in  $\Omega$  with boundary condition  $u_j(y)|_{\partial\Omega} = y_j|_{\partial\Omega}$  for  $y = (y_1, y_2)$ . Then,  $v_j$  can be replaced with  $v_j = u_j - y_j$ . Hence, the eigenvectors of the effective conductivity can be computed and the main direction of anisotropy changes in terms of the frequency as shown in Fig. 4(b).

#### 4.2. Implementation of the inverse homogenization

Following [2], we use the following values:

- The size of cells:  $50 \mu\text{m}$ ;
- Ratio between membrane thickness and size of a cell:  $0.7 \times 10^{-3}$ ;
- Medium conductivity:  $0.5$  S/m;
- Membrane conductivity:  $10^{-8}$  S/m;
- Background inclusion conductivity:  $10^{-7}$  S/m;
- Membrane permittivity:  $3.5 \times 8.85 \times 10^{-12}$  F/m;
- Frequency band:  $\omega/2\pi \in [10^4; 10^9]$  Hz.

In this case, we have values of  $\beta(\omega)$  for  $\omega/2\pi \in [10^4; 10^9]$  in Fig. 5. We consider a sample medium as follows: the cells are elliptic in shape, with axes lengths  $\rho_C a_C$  and  $\rho_C b_C$ , with  $a_C b_C \pi = 1$ . The



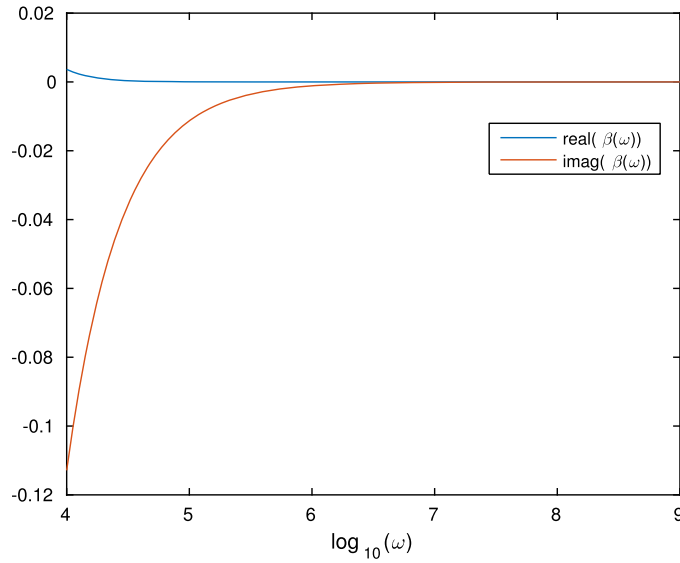


Fig. 5. Values of  $\beta(\omega)$  for  $\omega/2\pi \in [10^4; 10^9]$ .

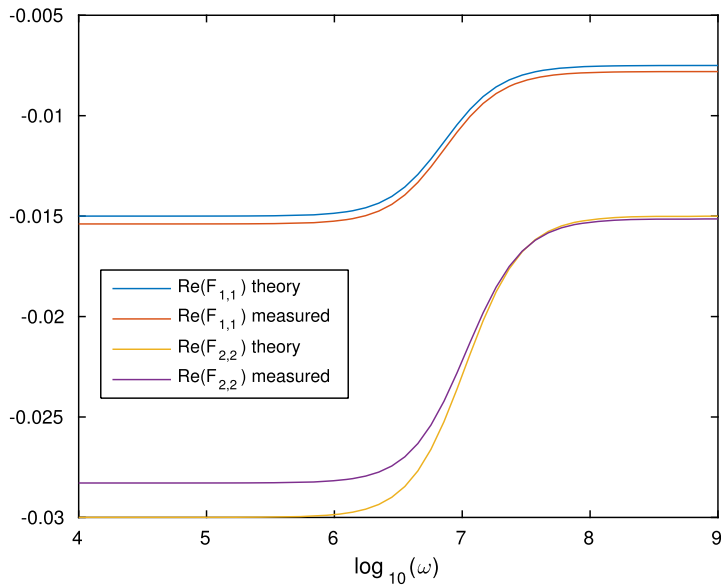


Fig. 6. Real part of the effective conductivity.

background is composed of elliptic inclusions, with axes lengths  $\rho_B a_B$  and  $\rho_B b_B$ , with  $a_B b_B \pi = 1$ . Their orientation is given by the angles  $\theta_C$  and  $\theta_B$  respectively.

At each frequency, in order to compute the true effective conductivity given by (5), we perform a finite element computation using freefem++ [7]. Comparison between the true effective conductivity and the expansion from Theorem 9 can be seen in Figs 6 and 7, in the case  $\theta_B = 0$  and  $\theta_C = 0$ , and  $\rho_B = \rho_C = 0.1$ .

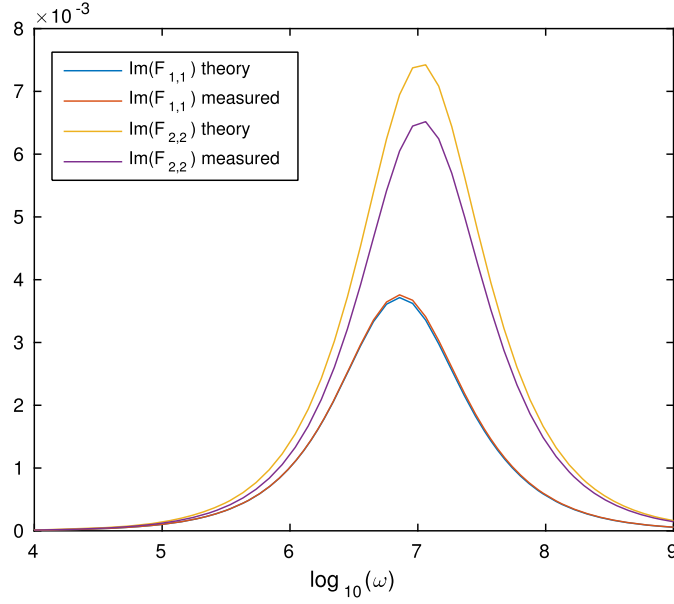


Fig. 7. Imaginary part of the effective conductivity.

To recover the moments from the effective conductivity, we approximate as a rational function,

$$F_{p,q}(z) \simeq \frac{p_0 + p_1z + \cdots + p_Nz^N}{q_0 + q_1z + \cdots + q_Nz^N}$$

for some  $N \in \mathbb{N}$ . Such an approximation of  $F$  is called a Padé approximation of  $F$ . Then we approximate the moments by the following values:

$$\begin{aligned} \tilde{a}_{0,p,q} &= \frac{p_0}{q_0}, \\ \tilde{a}_{1,p,q} &= \frac{p_1}{q_0} - \frac{q_1 p_0}{q_0^2}. \end{aligned}$$

Numerically, this is done as a simple least square inversion: the coefficients of the polynomials  $P(z) = p_0 + p_1z + \cdots + p_Nz^N$  and  $Q(z) = q_0 + q_1z + \cdots + q_Nz^N$  are computed to minimize the quantity

$$\sum_{k=1}^K \left| F_{p,q}(z_k) - \frac{P(z_k)}{Q(z_k)} \right|^2,$$

where  $z_1, \dots, z_K$  are the frequency values where  $F$  is measured.

We now consider a toy example where  $C$  is an ellipse in  $\mathbb{R}^2$ . In this case, if  $\lambda_1$  and  $\lambda_2$  are the eigenvalues of  $A_1$  defined by (20) for  $k = 1$ , the ratio  $r := \lambda_2/\lambda_1$  is independent of the volume fraction and is

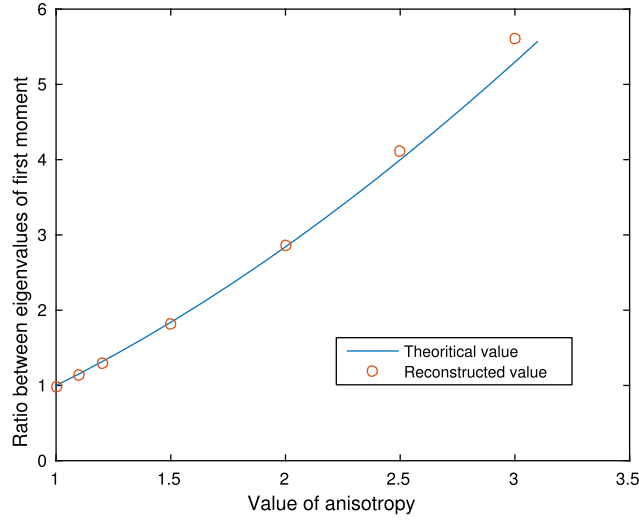


Fig. 8. Reconstruction of  $r$  when there is no inclusion  $B$ .

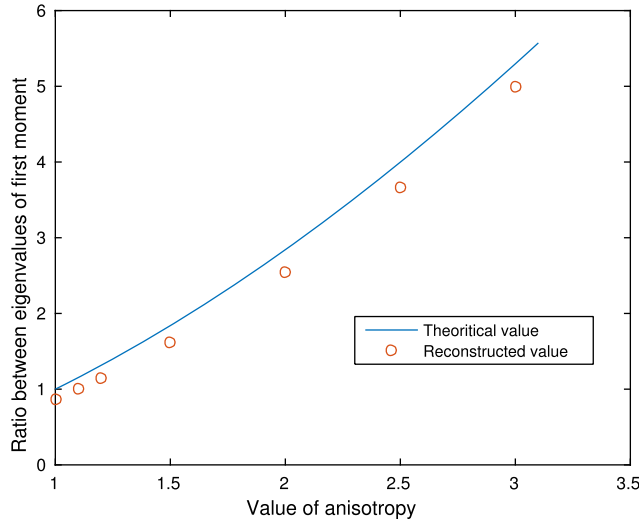


Fig. 9. Reconstruction of  $r$  when there is an inclusion  $B$  with  $\rho_B = 0.1$ .

given by

$$r = \frac{\int_0^{2\pi} \frac{b^2 \cos^2(t)}{\sqrt{b^2 \cos^2(t) + a^2 \sin^2(t)}} dt}{\int_0^{2\pi} \frac{a^2 \sin^2(t)}{\sqrt{b^2 \cos^2(t) + a^2 \sin^2(t)}} dt} = \frac{b \int_0^{2\pi} \frac{\cos^2(t)}{\sqrt{\cos^2(t) + \frac{a^2}{b^2} \sin^2(t)}} dt}{a \int_0^{2\pi} \frac{\sin^2(t)}{\sqrt{\frac{b^2}{a^2} \cos^2(t) + \sin^2(t)}} dt}. \quad (21)$$

Since the right-hand side of (21) can be regarded as a function of  $a/b$ , the anisotropy ratio  $a/b$  can be easily obtained by solving (21) with the known value  $r$ . In Fig. 8 (resp. in Fig. 9), we illustrate the reconstruction of the ratio  $r$  using the Padé approximation of  $F$  as a function of the anisotropy ratio  $a/b$

Table 1  
Reconstructed values of  $\rho_C$  with anisotropy ratio of 2

Values of $\rho_C$	0.01	0.02	0.03	0.05	0.1	0.2	0.3
Reconstructed value	0.0098	0.0196	0.0294	0.0491	0.0981	0.1963	0.2945

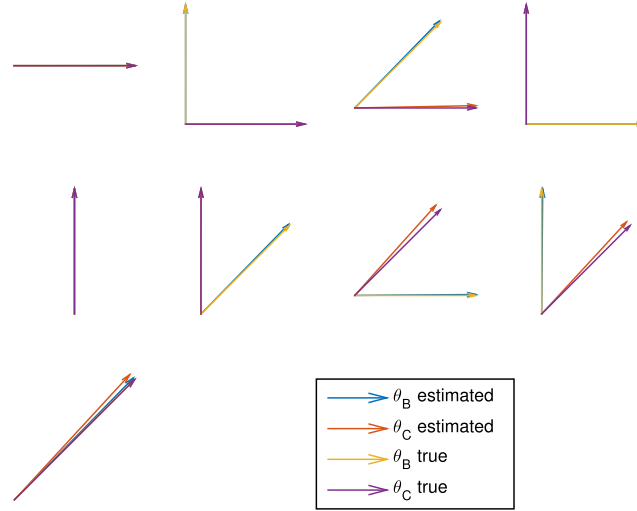


Fig. 10. Reconstruction of the orientation of the inclusions  $B$  and  $C$ .

compared to its theoretical value given by the preceding formula in the case where there is no inclusion  $B$  (resp. with an inclusion  $B$  with  $\rho_B = 0.1$ ). As we can see, the reconstruction is almost perfect in the case where there is no inclusion, and there is a slight bias induced by the inclusion  $B$ .

After recovering the anisotropy ratio  $a/b$ , we can recover the volume fraction  $\rho_C$  from the product of  $\lambda_1, \lambda_2$  of the eigenvalues of  $A_1$ . Indeed, we have

$$\begin{aligned} \lambda_1 \lambda_2 &= \rho_C^4 ab \int_0^{2\pi} \frac{\cos^2(t)}{\sqrt{\cos^2(t) + \frac{a^2}{b^2} \sin^2(t)}} dt \int_0^{2\pi} \frac{\sin^2(t)}{\sqrt{\frac{b^2}{a^2} \cos^2(t) + \sin^2(t)}} dt \\ &= \frac{\rho_C^4}{\pi} \int_0^{2\pi} \frac{\cos^2(t)}{\sqrt{\cos^2(t) + \frac{a^2}{b^2} \sin^2(t)}} dt \int_0^{2\pi} \frac{\sin^2(t)}{\sqrt{\frac{b^2}{a^2} \cos^2(t) + \sin^2(t)}} dt. \end{aligned}$$

Table 1 presents numerical reconstruction of the volume fraction  $\rho_C$  using the preceding formula, with an anisotropy ratio equal to 2.

To reconstruct the angle of the inclusions, we simply use the orientation of the eigenvalues of the moments of  $A_0$  for  $B$  and  $A_1$  for  $C$ . This is illustrated by results in Fig. 10 when both  $B$  and  $C$  are ellipses of anisotropy ratio 2 and with  $\rho_B = \rho_C = 0.1$ .

## Appendix. Spectrum of some periodic integral operators

Let  $C \subset \mathbb{R}^d$  be a  $C^{1+\alpha}$ -domain for some  $\alpha > 0$ . It is known that the non periodic operator  $\lambda I - \mathcal{K}_C^*$  is invertible on  $H^{-1/2}$  for  $\lambda \notin (-\frac{1}{2}, \frac{1}{2}]$  [4,6]. The positivity of  $\mathcal{L}_C$  [12, Section 3.3] also implies that

$\lambda\mathcal{I} + \mathcal{L}_C : H^{1/2} \rightarrow H^{-1/2}$  is invertible for  $\lambda > 0$ . We extend these results to the case of periodic Green's function.

**Theorem 16.** *For any  $\lambda > 0$ , the operator  $\lambda\mathcal{I} + \mathcal{L}_{\#,C} : H^{1/2}(\partial C) \rightarrow H^{-1/2}(\partial C)$  is invertible.*

**Proof.** We first show that the operator  $\mathcal{L}_{\#,C}$  is a Fredholm operator. Note that,  $\mathcal{L}_{\#,C} = \mathcal{L}_C + \mathcal{R}$  where  $\mathcal{R}$  is an integral operator with a smooth kernel and is therefore compact. Moreover, since  $\mathcal{L}_C$  has a dimension 1 kernel and image, it is a Fredholm operator. Therefore,  $\mathcal{L}_{\#,C}$  is Fredholm. Now we show that  $\mathcal{L}_{\#,C}$  is positive semi-definite, and the result will follow from the Fredholm alternative. Since

$$\langle \mathcal{L}_{\#,C}[\varphi], \psi \rangle_{L^2} = -\langle \mathcal{S}_{\#,C}[\text{curl}_{\partial C}\varphi], \text{curl}_{\partial C}\psi \rangle_{L^2}$$

for any  $\varphi, \psi \in H^{1/2}(\partial C)$ , we just have to show that  $\mathcal{S}_{\#,C}$  is negative semi-definite. From the expression (12) for  $G_{\#}$ , we compute, for any  $\varphi \in L^2(\partial C)$ ,

$$\begin{aligned} \langle \mathcal{S}_{\#,C}[\varphi], \varphi \rangle_{L^2} &= - \sum_{n \in \mathbb{Z}^d \setminus \{0\}} \int_{\partial C} \int_{\partial C} \frac{e^{2i\pi n \cdot (x-y)}}{4\pi^2 |n|^2} \varphi(x) \varphi(y) ds(x) dS(y) \\ &= - \sum_{n \in \mathbb{Z}^d \setminus \{0\}} \left( \int_{\partial C} \frac{e^{2i\pi n \cdot y}}{2\pi |n|} \varphi(y) dS(y) \right) \overline{\left( \int_{\partial C} \frac{e^{2i\pi n \cdot x}}{2\pi |n|} \varphi(x) ds(x) \right)} \\ &= - \sum_{n \in \mathbb{Z}^d \setminus \{0\}} \left| \int_{\partial C} \frac{e^{2i\pi n \cdot y}}{2\pi |n|} \varphi(y) dS(y) \right|^2 \leq 0. \end{aligned}$$

Therefore,  $\mathcal{S}_{\#,C}$  is negative semi-definite, which concludes the proof.  $\square$

**Theorem 17.** *For  $\lambda \notin (-\frac{1}{2}, \frac{1}{2}]$ , the operator  $\lambda I - \mathcal{K}_{\#,C}^*$  is invertible on  $H^{-1/2}(\partial C)$ .*

**Proof.** Since  $\lambda I - \mathcal{K}_C^*$  is invertible,  $\mathcal{K}_{\#,C}^* - \mathcal{K}_C^*$  is a compact operator [3],  $\lambda I - \mathcal{K}_{\#,C}^*$  is a Fredholm operator and it is enough to show that it is one-to-one. The proof goes exactly as in [4]. Let us assume that  $\lambda I - \mathcal{K}_{\#,C}^*$  is not one-to-one. Then there exists some  $f \in H^{-1/2}(\partial C)$  such that

$$(\lambda I - \mathcal{K}_{\#,C}^*)[f] = 0.$$

Let us write

$$(\lambda I - \mathcal{K}_{\#,C}^*)[f] = \left( \lambda - \frac{1}{2} \right) f + \left( \frac{1}{2} I - \mathcal{K}_{\#,C}^* \right)[f].$$

Since  $\langle (\frac{1}{2} I - \mathcal{K}_{\#,C}^*)[f], 1 \rangle_{L^2} = 0$ , we have  $\langle f, 1 \rangle_{L^2} = 0$ . Let  $u = \mathcal{S}_{\#,C}[f] \in H^1(\mathcal{Y} \setminus \partial C)$ . Let

$$A = \int_C |\nabla u(x)|^2 dx \quad \text{and} \quad B = \int_{\mathcal{Y} \setminus C} |\nabla u(x)|^2 dx.$$

Then  $A \neq 0$  or  $B \neq 0$  since  $f$  is not identically zero. Then by Green's formula together with the jump formulas, we have

$$A = \left\langle \left( -\frac{1}{2}I + \mathcal{K}_{\#,C}^* \right) [f], \mathcal{S}_{\#,C}[f] \right\rangle_{L^2} \quad \text{and} \quad B = \left\langle \left( \frac{1}{2}I + \mathcal{K}_{\#,C}^* \right) [f], \mathcal{S}_{\#,C}[f] \right\rangle_{L^2}.$$

Since  $(\lambda I - \mathcal{K}_{\#,C}^*)[f] = 0$ , we have  $\beta = \frac{1}{2} \frac{B-A}{B+A}$ . We have therefore a contradiction: we have  $|\beta| \leq \frac{1}{2}$  since  $A, B \geq 0$ . Therefore,  $\beta = -\frac{1}{2}$  which implies that  $B = 0$ . Therefore,  $u$  is constant in  $\mathbb{R}^d \setminus \bigcup_{n \in \mathbb{Z}^d} \{C + n\}$ . Since  $u$  is continuous across  $\partial C$ ,  $u$  is harmonic on  $C$  and is constant on  $\partial C$ , and by uniqueness of the Dirichlet problem on  $C$ ,  $u$  is constant on  $C$ . Therefore,

$$f = \frac{\partial}{\partial \nu} \mathcal{S}_{\#,C}[f] \Big|_+ - \frac{\partial}{\partial \nu} \mathcal{S}_{\#,C}[f] \Big|_- = 0,$$

which is a contradiction.  $\square$

## Acknowledgement

This work was supported by the ERC Advanced Grant Project MULTIMOD–267184.

## References

- [1] G. Allaire, Homogenization and two-scale convergence, *SIAM J. Math. Anal.* **23** (1992), 1482–1518. doi:[10.1137/0523084](https://doi.org/10.1137/0523084).
- [2] H. Ammari, J. Garnier, L. Giovangigli, W. Jing and J.K. Seo, Spectroscopic imaging of a dilute cell suspension, *J. Math. Pures Appl.* **105** (2016), 603–661. doi:[10.1016/j.matpur.2015.11.009](https://doi.org/10.1016/j.matpur.2015.11.009).
- [3] H. Ammari and H. Kang, *Polarization and Moment Tensors. With Applications to Inverse Problems and Effective Medium Theory*, Applied Mathematical Sciences, Vol. 162, Springer, New York, 2007.
- [4] T.K. Chang and K. Lee, Spectral properties of the layer potentials on Lipschitz domains, *Illinois J. Math.* **52** (2008), 463–472.
- [5] E. Cherkaev, Inverse homogenization for evaluation of effective properties of a mixture, *Inverse Prob.* **17** (2001), 1203–1218. doi:[10.1088/0266-5611/17/4/341](https://doi.org/10.1088/0266-5611/17/4/341).
- [6] E.B. Fabes, M. Sand and J.K. Seo, The spectral radius of the classical layer potentials on convex domains, in: *Partial Differential Equations with Minimal Smoothness and Applications*, Chicago, IL, 1990, IMA Vol. Math. Appl., Vol. 42, Springer, New York, 1992, pp. 129–137. doi:[10.1007/978-1-4612-2898-1\\_12](https://doi.org/10.1007/978-1-4612-2898-1_12).
- [7] F. Hecht, New development in freefem++, *J. Numer. Math.* **20** (2012), 251–266.
- [8] A. Khelifi and H. Zribi, Asymptotic expansions for the voltage potentials with two-dimensional and three-dimensional thin interfaces, *Math. Meth. Appl. Sci.* **34** (2011), 2274–2290.
- [9] S. Kim, E.J. Lee, E.J. Woo and J.K. Seo, Asymptotic analysis of the membrane structure to sensitivity of frequency-difference electrical impedance tomography, *Inverse Problems* **28** (2012), 075004. doi:[10.1088/0266-5611/28/7/075004](https://doi.org/10.1088/0266-5611/28/7/075004).
- [10] J.M. Mansour, Biomechanics of cartilage, in: *Kinesiology: The Mechanics and Pathomechanics of Human Movement*, Wolters Kluwer, Philadelphia, 2003, pp. 66–79.
- [11] G.W. Milton, *The Theory of Composites*, Cambridge Monographs on Applied and Computational Mathematics, Cambridge University Press, Cambridge, 2001.
- [12] J.-C. Nédélec, *Acoustic and Electromagnetic Equations – Integral Representations for Harmonic Problems*, Applied Mathematical Sciences, Vol. 144, Springer, Berlin, 2001.
- [13] G. Nguetseng, A general convergence result for a functional related to the theory of homogenization, *SIAM J. Math. Anal.* **20** (1989), 608–623. doi:[10.1137/0520043](https://doi.org/10.1137/0520043).
- [14] C. Orum, E. Cherkaev and K.M. Golden, Recovery of inclusion separations in strongly heterogeneous composites from effective property measurements, *Proc. Royal Soc. A* **468** (2012), 784–809. doi:[10.1098/rspa.2011.0527](https://doi.org/10.1098/rspa.2011.0527).

- [15] C. Poignard, Asymptotics for steady state voltage potentials in a bidimensional highly contrasted medium with thin layer, *Math. Meth. Appl. Sci.* **31** (2008), 443–479. doi:[10.1002/mma.923](https://doi.org/10.1002/mma.923).
- [16] C. Poignard, About the transmembrane voltage potential of a biological cell in time-harmonic regime, *ESAIM:Proceedings* **26** (2009), 162–179. doi:[10.1051/proc/2009012](https://doi.org/10.1051/proc/2009012).
- [17] J.K. Seo, T.K. Bera, H. Kwon and R. Sadleir, Effective admittivity of biological tissues as a coefficient of elliptic PDE, *Comput. Math. Meth. Medicine* **2013** (2013), 353849.
- [18] T. Zhang, T.K. Bera, E.J. Woo and J.K. Seo, Spectroscopic admittivity imaging of biological tissues: Challenges and future directions, *J. KSIAM* **18**(2) (2014), 77–105.